

Synthesis of Palladium Nanoparticles on Citrate-functionalized Graphene Oxide with High Catalytic Activity for 4-Nitrophenol Reduction

Bingyuan Su,¹ Yuzhu Jia,¹ Shuqiong Zhang,^{*1} Xiaomei Chen,^{*2,3} and Munetaka Oyama³

¹Xiamen Center for Disease Control and Prevention, Xiamen 361021, P. R. China

²College of Biological Engineering, Jimei University, Xiamen 361021, P. R. China

³Department of Material Chemistry, Graduate School of Engineering, Kyoto University, Nishikyō-ku, Kyoto 615-8520

(E-mail: xmchen@jmu.edu.cn)

Ultrafine Pd nanoparticles homogeneously deposited on citrate-functionalized graphene oxide (PdNPs/Cit-GO) were synthesized by a simple method with the reduction of ascorbic acid. The average size of these PdNPs was 4.67 nm, and they dispersed on the GO surface with high density. Significantly, the as-prepared PdNPs/Cit-GO expresses a high catalytic activity in the reduction of 4-nitrophenol (4-NP). The synergistic effect of the PdNPs/Cit-GO in the catalysis reaction was also demonstrated.

Palladium nanoparticles (PdNPs) are attracting tremendous attention owing to their versatile applications such as the hydrogenation of organic compounds, reduction of pollutants emitted from automobiles, and facilitation of coupling reactions.^{1–3} Because of the high cost and limited supply, it is important to maximize the activity of PdNPs while simultaneously decreasing the required amount of Pd by developing advanced morphologies and compositions. Because the activity of PdNPs is strongly related to their size and distribution, well-distributed PdNPs with small size and narrow distribution are ideal for achieving high catalytic activity. However, as the particle size is reduced, the surface energy of NPs increases, making them unstable with high tendency for interparticle aggregation. This will severely hinder the applications of PdNPs. For example, the aggregation of PdNPs will greatly reduce their specific surface area and consequently lower the catalytic efficiency.

In order to solve the problem of agglomeration and reduce the cost of Pd-based catalysts, PdNPs have been immobilized onto various supports.^{4–6} Among these supports, graphene oxide (GO) has received considerable interest because of their abundant functional groups, which can be used as the anchoring sites for metal NPs.⁷ Although more examples of GO–Pd hybrid synthesis have been demonstrated to date, only a few of them succeeded in preparing PdNPs with ultrafine size and well dispersion on the surface of GO.^{8–11} On the other hand, as a famous catalyst, most of these GO–Pd hybrids have been used as electrocatalysts, and as far as we know, there are no reports concerning the application of GO–Pd hybrids in the reduction of 4-nitrophenol (4-NP).

Herein, we reported a facile route to prepare well-distributed PdNPs with small size, high density, and narrow distribution on citrate-functionalized GO (PdNPs/Cit-GO). GO was prepared according to a modified Hummer's method¹² (see more details in the Supporting Information).¹³ First, 25 mg of GO was dispersed in 100 mL of water to obtain a yellow-brown aqueous solution with the aid of ultrasonication. In a typical synthesis of PdNPs/Cit-GO, Cit-GO was first prepared by adding 100 mg of sodium

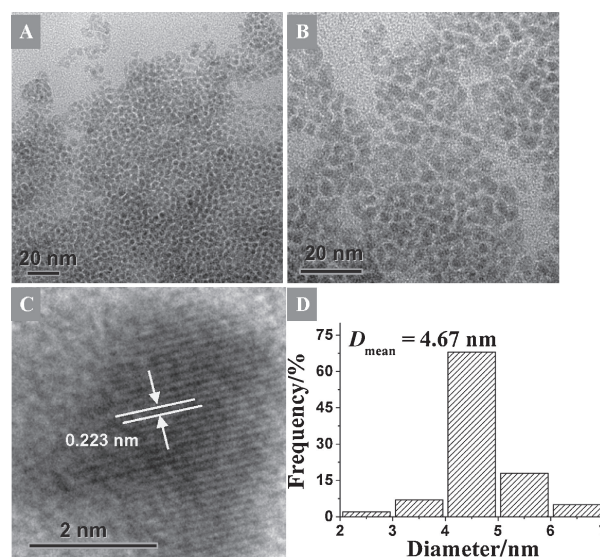


Figure 1. (A and B) Representative TEM and (C) HRTEM images of PdNPs/Cit-GO. (D) The histogram of particle size distribution of PdNPs/Cit-GO.

citrate into 10 mL of 0.25 mg mL⁻¹ of GO dispersion, followed by stirring for 12 h. Then, 0.5 mL of the as-prepared Cit-GO suspension, 0.25 mL of 10 mM K₂[PdCl₄], 0.05 mL of 1.0-M NaOH, and 0.05 mL of 0.1 M ascorbic acid (AA) were mixed in a vial under vigorous stirring for 2 h at room temperature. The color changed from orange to black in 10 min after the addition of AA. Finally, the product was centrifuged and washed to remove the remaining reagents.

Figures 1A–1C show the typical TEM images of the product at different magnifications. The low-magnification TEM images (Figures 1A and 1B) display that the as-prepared PdNPs have high density and are well dispersed on the surface of GO. The high-resolution TEM image (HRTEM) (Figure 1C) indicates that each PdNPs presented a single-crystalline structure. The interplanar spacing is 0.223 nm, which agrees well with the (111) lattice spacing of face-centered cubic (fcc) Pd (0.224 nm). The histogram of the particle-size distribution in Figure 1D indicates that most of the PdNPs are in the range 4–5 nm, and the average size was 4.67 nm. Moreover, the relative standard deviation (RSD) of these NPs' size is 6.2%, suggesting the well dispersion of these PdNPs.

Figure 2A shows a typical EDX analysis of the prepared PdNPs/Cit-GO, in which obvious Pd peaks could be found, suggesting that the PdNPs were successfully attached onto the GO surface. The PdNPs/Cit-GO was further characterized

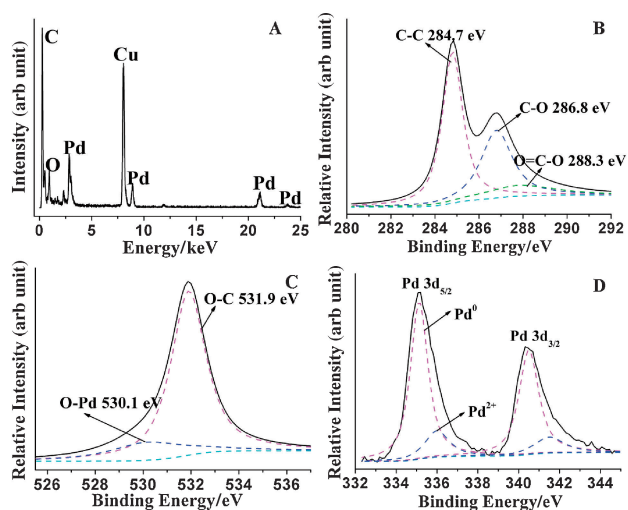


Figure 2. (A) EDX analysis of PdNPs/Cit-GO. (B–D) XPS spectra of C1s, O1s, and Pd3d on PdNPs/Cit-GO with deconvolution results.

by XPS measurements to investigate the surface nature. Figures 2B–2D show the deconvoluted XPS spectra of C1s, O1s, and Pd3d. Comparing with the binding energy of C1s on a GO surface,⁸ after the reaction, the peak of C–O (286.8 eV) was reduced (Figure 2B), probably because of the weak reduction of AA. This weak reduction can also be supported by the remaining obvious O1s spectra in Figure 2C. Figure 2D shows the deconvoluted XPS spectra of Pd3d, in which the relative intensities of the different Pd species are also given. It is interesting to note that a considerable percentage of Pd was in its native state (Pd⁰, 74%) in PdNPs/Cit-GO, which corresponded to the weak peak of Pd–O (530.1 eV) in the deconvolution of O1s spectra. Additionally, from the XPS data, the Pd content was estimated to be 23 wt%.

The catalytic activity of PdNPs/Cit-GO is tested by the reduction of 4-NP to 4-aminophenolate (4-AP) in the presence of NaBH₄. The reaction process was monitored by UV–vis spectrometry, as illustrated in Figure 3. 4-NP reveals a peak at 316 nm, after the addition of NaBH₄, the color quickly changed from light yellow to yellow-green, and in the UV–vis absorption spectra, a strong absorption peak shifted from 316 to 400 nm, suggesting the formation of 4-nitrophenolate anions under alkaline conditions (Figure 3A). Nevertheless, the absorbance at 400 nm remained unchanged with time, indicating that it was difficult for the reduction to proceed without a catalyst. Moreover, upon the addition of Cit-GO, there was still no obvious change in the absorbance at 400 nm in 60 min (Figure 3B), which was different from those of Pd/C (20 wt%, Aldrich Chem Co., see more details in Figure S1) and PdNPs/Cit-GO. As shown in Figures 3C and 3D, the absorption of 4-nitrophenolate anions at 400 nm decreases along with a concomitant increase of the 302 nm peak of 4-AP, and an isosbestic point can be observed at 322 nm, suggesting that the catalytic reduction of 4-NP afforded only 4-AP, without any other by-product.¹¹ Moreover, it should be mentioned that compared with Pd/C, the PdNPs/Cit-GO exhibited a faster reaction rate with a shorter time to complete the reaction, indicating a higher catalytic activity of PdNPs/Cit-GO for the reduction of 4-NP.

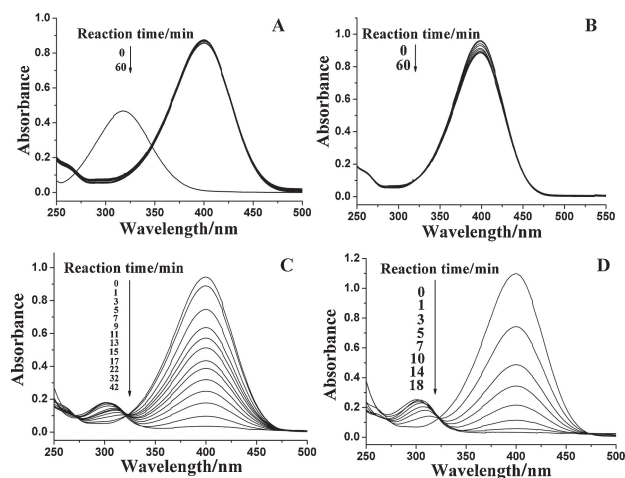


Figure 3. UV–vis spectra of (A) 4-NP before and after addition of NaBH₄ solution, (B–D) Time-dependent UV–vis absorption spectra of reduction 4-NP by NaBH₄ in presence of (B) Cit-GO, (C) Pd/C, and (D) PdNPs/Cit-GO.

Table 1. Summary of the weight percentage of Pd (based on XPS results) and the rate constants of the catalysts

Sample	Preparation approach		Pd/wt %	k_{app}/s^{-1}^a	$\kappa/s^{-1}g^{-1}b$
	Cit-GO /mL	K ₂ [PdCl ₄] /mL			
1	0.5	0.125	17	0.0024	483.3
2	0.5	0.25	23	0.0033	656.7
3	0.5	0.5	29	0.0020	400.0
4	0.5	0.75	32	0.0015	303.3
Pd/C	—	—	20	0.0014	273.3

^a k_{app} was calculated on the basis of $\ln(A_t/A_0) = -k_{app}t$. ^b κ was calculated by $\kappa = k_{app}/m_{Pd}$.

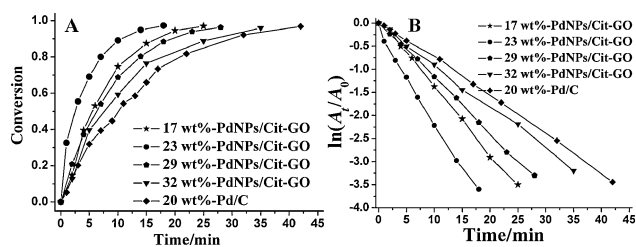


Figure 4. (A) Time-dependent conversion of 4-NP reduction catalyzed by different catalysts. (B) Plot of $\ln(A_t/A_0)$ versus time for the reduction of 4-NP over different catalysts.

Further studies were performed to investigate the synergistic effect on the delivery of electrons between GO and PdNPs. By varying the amount of [PdCl₄]²⁻ in the synthesis, a series of PdNPs/Cit-GO with Pd contents in the range 17–32% were obtained (Table 1). The catalytic behaviors of these PdNPs/Cit-GO composites were studied under the same conditions. Figure 4A shows the time-dependent conversion of 4-NP reduction catalyzed by different catalysts (the amount of catalyst was controlled at 5 μ g of Pd). Compared with the other catalysts, the reaction proceeds rapidly with the conversion exceeding 90% at a time of 10 min upon the addition of PdNPs/Cit-GO

with 23 wt % Pd content (23 wt %-PdNPs/Cit-GO). Because the concentration of BH_4^- is much higher than that of 4-NP, the reaction rate could be regarded to be independent of the BH_4^- concentration. Thus, pseudo-first-order kinetics was used to evaluate the rate of the catalytic reaction. As expected, linear relationships of $\ln(A_t/A_0)$ versus reaction time were obtained (Figure 4B), where A_t and A_0 represent the absorbance at the intervals and the initial stage of 4-nitrophenolate anions, respectively. Obviously, all the PdNPs/Cit-GO exhibited a larger rate constant (k_{app}) than that of Pd/C, suggesting a stronger synergistic effect of electron delivery between GO and PdNPs. Moreover, among all these catalysts, 23 wt %-PdNPs/Cit-GO show the largest rate constant at 0.0033 s^{-1} , which indicated that the electron transfer (from BH_4^- to 4-NP) at the 23 wt %-PdNPs/Cit-GO surface is faster than the others. To better compare the performance of our catalyst with other reported materials, we summarized the rate constant of these catalysts in Table S1. It is clear that the PdNPs/Cit-GO showed either comparable or even better performance for the reduction of 4-NP. Additionally, because of the direct effect of the used catalyst concentration on the rate constant, the parameter $\kappa = k_{\text{app}}/m_{\text{Pd}}$, which is the ratio of the rate constant k_{app} to the Pd weight of the catalyst was used to estimate the catalytic performance of different catalysts. For our catalyst, κ was at $656.7 \text{ s}^{-1} \text{ g}^{-1}$, which is much larger than those of the reported catalysts such as PdNPs on porous carbon spheres ($14.6 \text{ s}^{-1} \text{ g}^{-1}$),¹⁴ Ag dendrites ($8.6 \text{ s}^{-1} \text{ g}^{-1}$),¹⁴ and Pd–Ag NPs ($8.3 \text{ s}^{-1} \text{ g}^{-1}$).¹⁵ As the diffusion rate of 4-NP and 4-AP plays an important role in the reaction,¹⁶ the large rate constant also illustrated that the PdNPs on 23 wt %-PdNPs/Cit-GO are largely exposed to water without coating Cit; hence, 4-NP diffusion to PdNPs and 4-AP diffusion away from PdNPs are not hindered. From these observations, it is clear that 23 wt %-PdNPs/Cit-GO showed the highest catalytic ability toward the reduction of 4-NP.

In summary, we synthesize PdNPs/Cit-GO composite by a simple one-pot method. By varying the amounts of Pd precursor, the content of Pd supported on Cit-GO could be flexibly tuned. Moreover, the PdNPs/Cit-GO composite exhibited high catalytic activity in the reduction of 4-NP. The synergistic effect of the electron delivery in the catalysis reaction was also demonstrated. Moreover, the 23 wt %-PdNPs/Cit-GO showed the highest catalytic activity among all the catalysts for the reduction of 4-NP. In the light of these unique characteristics, the PdNPs/Cit-GO composite will find a wide range of new applications in environment chemistry and biochemistry.

Xiaomei Chen thanks the Japan Society for the Promotion of Science (JSPS) for the fellowship. This work was financially supported by the National Natural Science Foundation of China (No. 21305050), Special Foundation for Young researchers of the Health Department of Fujian (No. 2013-2-106), the Scientific Research Foundation of the Education Department of Fujian (No. FB2013006), and JSPS KAKENHI Grant Nos. 24•02335 and 24550100.

References and Notes

- H. Liu, T. Jiang, B. Han, S. Liang, Y. Zhou, *Science* **2009**, *326*, 1250.
- S. Sartipi, A. A. Khodadadi, Y. Mortazavi, *Appl. Catal., B* **2008**, *83*, 214.
- D. B. Pacardo, M. Sethi, S. E. Jones, R. R. Naik, M. R. Knecht, *ACS Nano* **2009**, *3*, 1288.
- X.-m. Chen, Z.-j. Lin, T.-t. Jia, Z.-m. Cai, X.-l. Huang, Y.-g. Jiang, X. Chen, G.-n. Chen, *Anal. Chim. Acta* **2009**, *650*, 54.
- A. V. Biradar, A. A. Biradar, T. Asefa, *Langmuir* **2011**, *27*, 14408.
- C.-M. Chang, M.-H. Hon, I.-C. Leu, *ACS Appl. Mater. Interfaces* **2013**, *5*, 135.
- X.-m. Chen, G.-h. Wu, Y.-q. Jiang, Y.-r. Wang, X. Chen, *Analyst* **2011**, *136*, 4631.
- X. Chen, G. Wu, J. Chen, X. Chen, Z. Xie, X. Wang, *J. Am. Chem. Soc.* **2011**, *133*, 3693.
- D. Kim, M. S. Ahmed, S. Jeon, *J. Mater. Chem.* **2012**, *22*, 16353.
- X. Liu, L. Li, C. Meng, Y. Han, *J. Phys. Chem. C* **2012**, *116*, 2710.
- T. Sun, Z. Zhang, J. Xiao, C. Chen, F. Xiao, S. Wang, Y. Liu, *Sci. Rep.* **2013**, *3*, 2527.
- L. J. Cote, F. Kim, J. Huang, *J. Am. Chem. Soc.* **2009**, *131*, 1043.
- Supporting Information is available electronically on the CSJ-Journal Web site, <http://www.csj.jp/journals/chem-lett/index.html>.
- S. Tang, S. Vongehr, G. He, L. Chen, X. Meng, *J. Colloid Interface Sci.* **2012**, *375*, 125.
- J. Huang, S. Vongehr, S. Tang, H. Lu, X. Meng, *J. Phys. Chem. C* **2010**, *114*, 15005.
- K. Esumi, R. Isono, T. Yoshimura, *Langmuir* **2004**, *20*, 237.